TISSUE ENGINEERING: Part A
Volume 17, Numbers 9 and 10, 2011

DOI: 10.1089/ten.tea.2010.0490

Orthodontic Tooth Movement in Alveolar Cleft Repaired with a Tissue Engineering Bone: An Experimental Study in Dogs

Dongjie Zhang, MDSc,[1] Fengting Chu, MDSc,[1] Yan Yang, MDSc,[1] Lunguo Xia, Ph.D.,[2] Deliang Zeng, MDSc,[2] Hasan Uludağ, Ph.D.,[3] Xiuli Zhang, B.D.S.,[2] Yufen Qian, MDSc,[1] and Xinquan Jiang, Ph.D.[2]

Tissue engineering approaches have been successfully used in repairing bone defects and have become a viable alternative to autologous bone. The aim of the present study was to investigate if a construct of porous beta-tricalcium phosphate (β-TCP) combined with osteogenically induced bone marrow stromal cells (bMSCs) could repair alveolar cleft, and allow for subsequent orthodontic tooth movement in a canine model. Twelve alveolar osteotomy surgeries in six animals were made bilaterally and randomly implanted by (1) tissue-engineered bone complex of bMSCs/β-TCP (group A, $n=4$), (2) β-TCP alone (group B, $n=4$), and (3) autologous bone obtained from iliac bone (group C, $n=4$). Contralateral alveolar defects were created in one animal and left untreated to serve as blank control to observe spontaneous healing of the defects. Sequential fluorescent labeling and radiographic observation was used to evaluate new bone formation and mineralization in each defect. Orthodontic tooth movement was initiated 8 weeks after surgical operation for 12 weeks, and then the dogs were sacrificed for histological and histomorphometric analysis. Results indicated that the tissue-engineered complex with bMSCs/β-TCP dramatically promoted new bone formation and mineralization and achieved a favorable height of the repaired alveolar when compared with β-TCP alone, which absorbed severely. The overall effect of the tissue-engineered bone was equivalent to autologous bone; the physiological function of the alveolar bone was restored by allowing the adjacent teeth to move into the newly formed bone in the grafted region. This study demonstrated that the tissue engineering bone from the combination of β-TCP and bMSCs is a feasible clinical approach for patients with alveolar cleft and the subsequent orthodontic tooth movement.

Introduction

Alveolar cleft is a highly prevalent congenital malformation, where 75% of the patients with cleft lip and palate display osseous defects of the premaxilla alveolar bone.[1] To stabilize the periodontium of the teeth adjacent to the cleft and the maxillary dental arch, to close oronasal fistulae, and to improve facial and dental esthetics, secondary bone grafting is widely attempted under strict clinical protocol for treatment of alveolar cleft patients.[2,3] Orthodontic treatment could be initiated after bone grafting to align the dentition, move the adjacent teeth into the cleft, and improve midfacial retrusion that resulted from an unfavorable growth inhibition of the craniofacial complex.[4,5] Since it may present a limitation to orthodontist who would like to move teeth into the cleft region, favorable periodontal bone should be required to support the teeth to eliminate severe periodontal problems caused by attempts to move the teeth into the edentulous defects.[6]

Contemporary treatments of alveolar cleft defects involve surgical techniques that implant autologous bone grafts into the defect site.[7] Particulate cancellous bone harvested from the anterior iliac crest is most widely used for treating alveolar cleft and considered as the gold standard because of its osteoconductive, osteoinductive, and nonimmunogenic property.[8,9] This technique, however, has several disadvantages, including early complications such as pain, bleeding, wound infection at the harvest site, as well as poor mobility, and the possibility of a fracture. Late complications, including chronic pain, and unaesthetic scarring at the harvest site, as well as gait disturbance, and paresthesia.[10,11] Further, the autologous bone grafting has 15% or higher failure rates

[1]Department of Orthodontics and [2]Oral Bioengineering Lab, Shanghai Research Institute of Stomatology, Ninth People's Hospital Affiliated to Shanghai Jiao Tong University, School of Medicine, Shanghai Key Laboratory of Stomatology, Shanghai, China.
[3]Department of Chemical and Materials Engineering, University of Alberta, Edmonton, Canada.

(depending on evaluation criteria),[12,13] and increases the burden both for the patients and the healthcare system.

Tremendous efforts have been made to explore substitutes for autologous bone grafting. Numerous substitutes have been investigated, including the naturally derived biomaterials such as hyaluronic acid, and synthetic biomaterials such as hydroxyapatite (HA), beta-tricalcium phosphate (β-TCP), calcium phosphate ceramic, poly[D,L-(lactide-co-glycolide)], and collagen/HA composites.[14–18] These substitutes may possess favorable osteoconductive characteristics (i.e., stimulation of endogenous osteoblasts and/or progenitor cells to migrate into defect region), but their limitation is intrinsic osteogenesis ability that compromises the desired clinical outcome for repairing bone defects.[12] Bone marrow stromal cells (bMSCs), which can be isolated from bone marrow, have the ability to differentiate into osteoblasts and form new bone.[19,20] More importantly, it has been reported that bMSCs combined with scaffolds could repair bone defects in numerous animal models, including oral and maxillofacial defects.[21–23] As an alternative strategy to improve the final outcome of patients with cleft alveolar, a tissue engineering approach in which the biomaterial substitutes are combined with osteogenic cells is presented in this study. A few case reports have been reported to date using tissue engineering techniques for repairing alveolar cleft.[10,24,25] However, no adequate comparison of tissue engineering bone to autologous bone grafting was performed with regard to functional outcomes, such as moving of adjacent teeth to the grafted area to correctly line up the teeth. It is imperative to assess whether the newly formed bone would support the adjacent teeth beside the cleft to facilitate the orthodontic treatment. Thus, sequential systemic investigations are needed in preclinical models to explore if the newly formed bone could maintain the normal alveolar function.

In this study, we investigated the ability of a tissue-engineered bone. The tissue-engineered bone was fabricated by combining porous particulate β-TCP and autologous osteogenically induced bMSCs. We specifically explored if tissue-engineered bone in the alveolar cleft could function similarly to autologous bone grafting in terms of supporting the teeth movement adjacent to the cleft as a follow-up orthodontic procedure.

Materials and Methods

Animals

Seven 24-week-old male beagle dogs (weighing 8.0–9.5 kg) were used in this study. Twelve alveolar bone graft surgeries in six animals were made bilaterally and repaired randomly by the following three groups of materials—group A: tissue-engineered bone complex of bMSCs/β-TCP ($n=4$); group B: β-TCP alone ($n=4$); group C: autologous bone obtained from iliac bone ($n=4$). Bilateral alveolar defects in the rest of the animal were created and served as a blank control to observe if they could heal spontaneously during the experiment period. The experimental protocol was approved by the Animal Care and Experiment Committee of Ninth People's Hospital affiliated to Shanghai Jiao Tong University, School of Medicine.

Cell culture and osteogenic induction

Under general anesthesia with intramuscular ketamine (10 mg/kg), 3 mL of autologous bone marrow aspirate was obtained from the iliac crests of each dog with a heparinized 16 G biopsy needle and transferred into a sterile centrifuge tube. After washed with phosphate buffered saline (PBS) containing of 100 U/mL penicillin and 100 U/mL streptomycin, bone marrow samples were centrifuged at 1800 rpm for 10 min. Nucleated cells were seeded in 100 mm dishes in Dulbecco's modified Eagle's medium (Gibco) containing 10% (v/v) fetal bovine serum (FBS; Gibco), 100 U/mL penicillin, and 100 U/mL streptomycin, which was acted as a growth medium in present study, and incubated at 37°C under 95% humidity with 5% CO_2. Nonadherent cells were removed from the culture during the medium changes twice every week. When cell colonies reached 70%–80% confluence, cells were detached with 0.25% trypsin/ethylenediaminetetraacetic acid and passaged. From passage 1, cells for osteogenic induction were cultured in the osteogenic medium (Dulbecco's modified Eagle's medium supplemented with 10% FBS, 10^{-8} M dexamethasone, 10 mM β-phosphoglycerol, and 50 mM L-2-ascorbic acid; Sigma). The cells after second passages were used for the following studies.

Osteogenic differentiation of bMSCs cultured in the osteogenic medium

Alkaline phosphatase (ALP) staining was tested after 7 days of culture in the osteogenic medium. The cells were fixed for 10 min at 4°C and then incubated with a mixture of naphthol AS–MX phosphate and fast blue BB salt (ALP kit; Hongqiao) according to Zhao *et al.*[26] The alizarin red staining was performed after 21 days of culture under the osteogenic medium. The cells were fixed with 10% formalin and stained with 40 mM alizarin red solution for 30 min at 37°C.

For assessment of quantitative ALP activity, the assay was conducted after 4 and 7 days of culture in either the growth medium or the osteogenic medium.[27,28] Briefly, bMSCs in 24-well plates were washed twice with PBS and suspended in lysis buffer with 0.1 mL of 0.2% NP-40, and then the cells were mixed with 0.1 mL of 1 mg/mL p-nitrophenyl phosphate (Sigma) in 1 M diethanolamine buffer. After incubation at 37°C for 15 min, the reaction was stopped by the addition of 3 N NaOH. Enzyme activity was quantified by absorbance at 405 nm. Total protein content was determined with the Bradford method by using the Bio-Rad protein assay kit (Bio-Rad), and a series of bovine serum standards. ALP activity was normalized by the protein content and expressed as Abs/mg protein.

To detect mineralization, bMSCs on days 14 and 21 were washed five times in PBS and fixed in cold 70% ethanol for 1 h. The cells were washed three times with dH_2O and stained with 40 mM alizarin red solution for 20 min at room temperature, and then the stain was desorbed with 10% cetylpyridinium chloride (Sigma) for 1 h. Finally, the dye was collected and mineralization was quantified by absorbance at 590 nm (Elx800; Bio-Tek) as described in previous study.[29] All experiments were done in triplicate.

Quantitative real-time polymerase chain reaction (PCR) assay was performed for osteoblast gene expression by using bMSCs cultured in either the growth medium or the osteogenic medium. Total RNA was isolated from cells at days 4 and 7, by using Trizol reagent (Invitrogen) according to the manufacturer's instruction. The RNA was used for synthesizing complementary DNA (cDNA) with PrimeScript 1st Strand cDNA Synthesis kit (TaKaRa). Real-time PCR analy-

Table 1. Primer Sequences Used for Real-Time Polymerase Chain Reaction

Gene	*Primers (F, forward; R, reverse)*	*Accession numbers*	*Product size (bp)*
Runx2	F: 5′ACGATCTGAGATTTGTGGGC3′ R: 5′CGTCTCCAATAGGAAGGCAA3′	XM_845779.1	166
OPN	F: 5′CACTGACATTCCAGCAAC3′ R: 5′CTTCCATACTCGCACTTT3′	XM_535649.2	188
BSP	F: 5′TGGCTCTAAGACAACACTC3′ R: 5′TGTGCCCTTTATAGTAGCT3′	XM_846356.1	245
OCN	F: 5′TCACAGACCCAGACAGAACCG3′ R: 5′AGCCCAGAGTCCAGGTAGCG3′	XM_547536.2	207
GAPDH	F: 5′TTCGACAGTCAGCCGCATCTT3′ R: 5′ATCCGTTGACTCCGACCTTCA3′	XM_848580.1	79

BSP, bone sialoprotein; GAPDH, glyceraldehyde-3-phosphate dehydrogenase; OCN, osteocalcin; OPN, osteopontin; Runx2, runt-related transcription factor 2.

sis was performed with Bio-Rad real-time PCR system (MyiQ™; Bio-Rad) on markers of runt-related transcription factor 2 (Runx2), osteopontin (OPN), bone sialoprotein (BSP), and osteocalcin (OCN), with glyceraldehyde-3-phosphate dehydrogenase (GADPH) as the house-keeping gene for normalization. Primer sequences for Runx2, OPN, BSP, OCN, and GAPDH are listed in Table 1. All experiments were done in triplicate. The bMSCs cultured with the growth medium was used as a control.

Cell seeding and osteogenic differentiation of bMSCs on β-TCP scaffolds

Sterilized particulate porous β-TCP with a diameter of 1.5–2.5 mm (Shanghai Bio-Lu Biomaterials Co. Ltd.) was used as scaffold. Cells cultured in either the growth medium or the osteogenic medium were detached from culture dishes using 0.25% trypsin/ethylenediaminetetraacetic acid, centrifuged, and then re-suspended in the medium without FBS at a density of 2×10^7 cells/mL, and then bMSCs suspension was dropped onto the β-TCP by means of the pipetting technique and incubated in the 24-well plate at 37°C for 4 h as previously described.[30] The bMSCs/β-TCP constructs were then cultured in the growth medium or osteogenic medium, correspondingly. Cell spreading on the scaffolds was detected under scanning electron microscopy (SEM; Philips SEM XL-30) at 4 days after cell seeding. While the osteogenic differentiation of bMSCs on β-TCP scaffolds was analyzed with ALP activity assay, quantitative alizarin red mineralization analysis, and quantitative real-time PCR analysis on the osteogenic marker of Runx2, OPN, BSP, and OCN as previously described. The tissue-engineered bone constructing with osteogenically induced bMSCs and β-TCP scaffolds was used for grafting in surgically created alveolar cleft sites.

Surgical procedure

The maxillary third incisors were extracted bilaterally for all animals under general anesthesia through intramuscular injection of ketamine (10 mg/kg), whereas a standard monitoring of general anesthesia was performed, and anesthesia was maintained with intravenous administration of ketamine during the entire course of surgery. Vertical incisions about 15 mm were made on the labial gingiva and mucous between the mesial of the second incisor and the distal of the canine. Full-thickness mucoperiosteal flaps of the labial and palatal were elevated to expose the alveolar crests bone. Alveolar defects (10×5×15 mm) extending to the nasal floor were made bilaterally by a round carbide bur with physiologic saline cooling between the second incisor and canine (Fig. 1). Great care was taken to avoid penetrations to the nasal floor and injuries to the second incisors. Grafts from different groups were transplanted to repair the alveolar defects. For the autologous bone grafts, an incision of 5 cm was made on top of the anterior iliac crest and cortico-cancellus bone blocks were harvested. Then, the wound was closed in layers. The animals were injected with penicillin for 1 week and kept on a soft diet during the study.

Orthodontic tooth movement and measurement of the tooth movement

Orthodontic tooth movement (distal movement of the first lateral incisor) was initiated 8 weeks after surgical operation using a segmental arch wire (0.018×0.025 inch rectangular stainless steel; 3M Unitek) with a nickel–titanium closed coil spring between the first lateral incisor and the canine. The canine was banded and a buccal tube was welded to the band, and the first lateral incisor was bonded with a 0.022×0.028 inch slot bracket (Fig. 2A). An applied force of 50 *g* was used and every 2 weeks the appliances were adjusted to avoid arch wire distortion to maintain the set force level. To eliminate occlusal interference, the height of the mandibular incisors and canines were reduced by a trepan bar. Orthodontic tooth movement was lasted for another 12 weeks and the dogs were sacrificed at 20 weeks after surgical operation. The orthodontic tooth movement was recorded with a dental model and measured by using a three-dimensional laser scanner (Laser-RE600; SEREIN). Briefly, the scanned models (before and after orthodontic tooth movement) were aligned on the same plane that was determined by the mesial cusps of the second premolas and the cutting edge of the central incisors. Based on this plane, a coordinate was created using the midline of the palate as X-axis and the line through the mesial cusps of the second premolas as Y-axis. The distance of the first lateral incisor before and after orthodontic tooth movement to the X-axis and Y-axis was measured and recorded as (Dx, Dy) and (Dx′, Dy′) (Fig. 2C1, C2). The tooth displacement was calculated using the formula as follows: $D=\sqrt{(Dx'-Dx)^2+(Dy-Dy')^2}$ and compared.

Radiographic observation

Maxillary occlusal films were obtained with a dental X-ray machine (Trophy) under general anesthesia with ketamine as

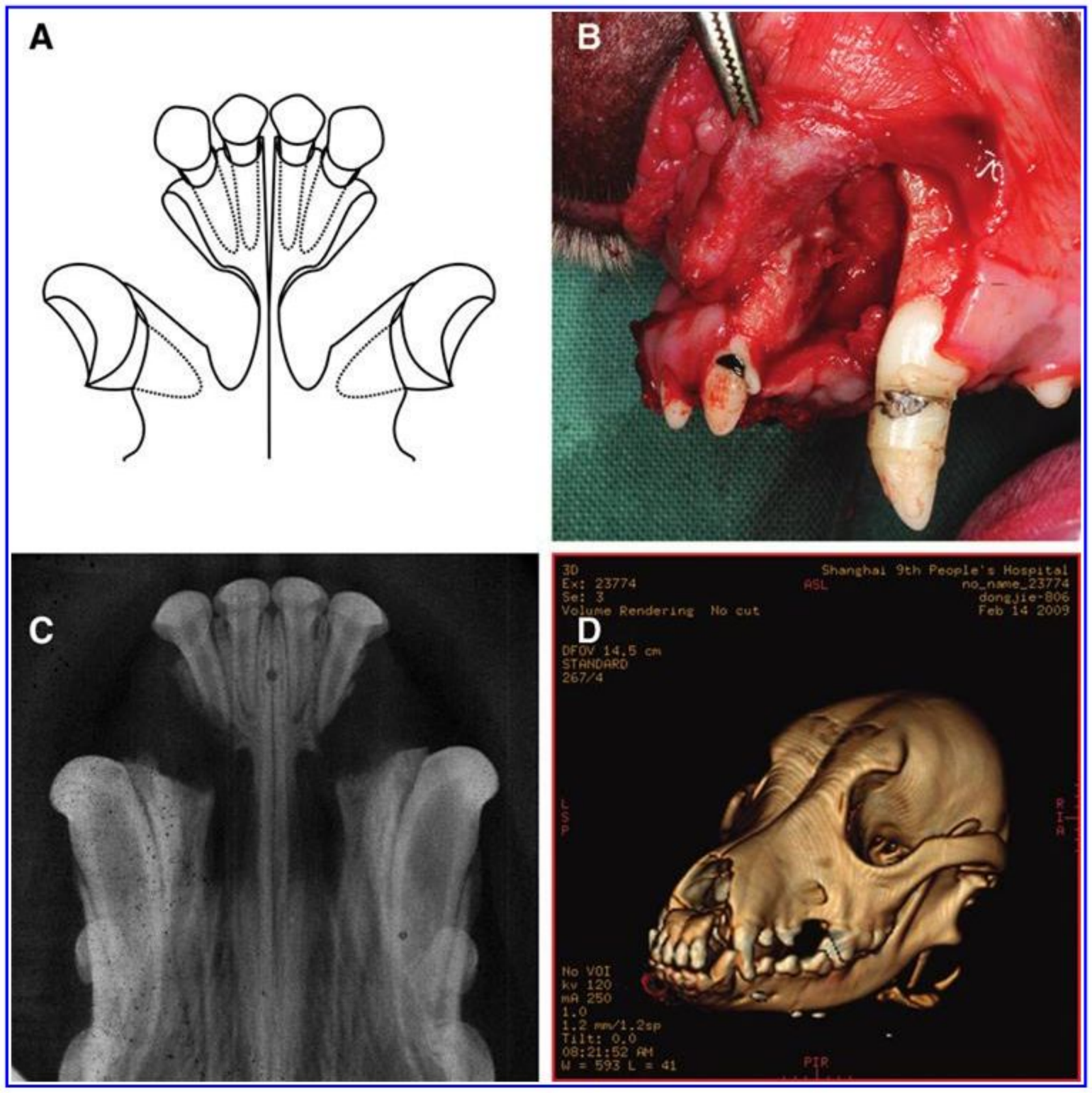

FIG. 1. Surgically created alveolar cleft model in dogs was illustrated. Scheme was drawn to show the size and shape of the surgically created alveolar cleft **(A)**. Photograph of the surgically created alveolar cleft was shown during surgery **(B)**. Occlusal view of the alveolar cleft was taken immediately after operation by X-ray **(C)**. Reconstructed three-dimensional computed tomogram of the alveolar cleft immediately after operation was shown by computer tomography **(D)**. Color images available online at www.liebertonline.com/tea

described previously, immediately after bone graft implantation, or at 4, 8, and 20 weeks after implantation, from a distance of 7 cm with an exposure time of 0.28 s (230 V, 8 mA). The height of the alveolar crest from each group was evaluated. Briefly, root length (from the enamelo-cemental junction to root apex) of the first lateral incisors in the occlusal films immediately after surgery and 20 weeks after implantation was measured, respectively, and recorded (L0, L1). L0/L1 ratio was calculated and adopted for the comparison to correct any possible projected deviations. Then,

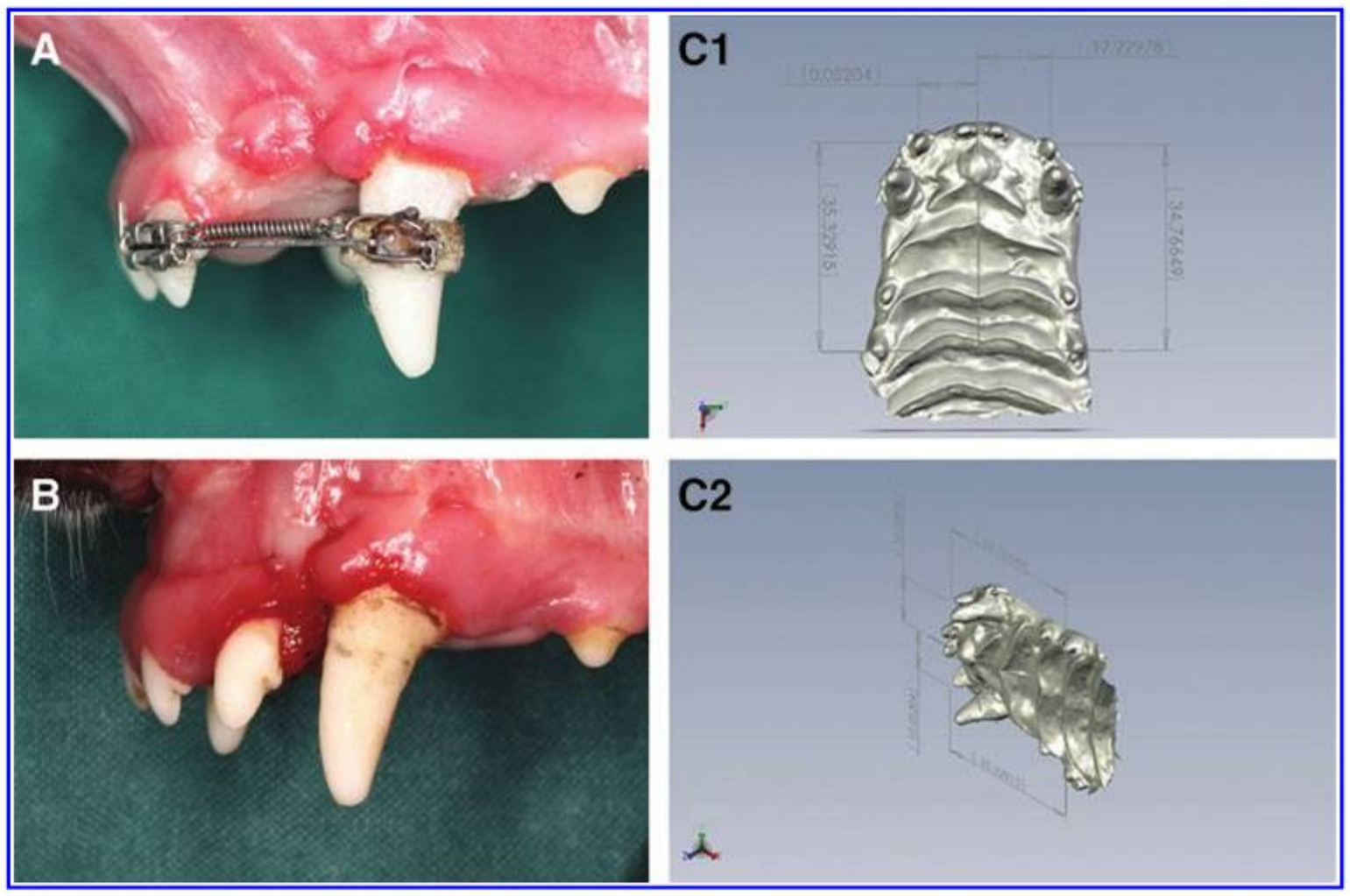

FIG. 2. Photograph of orthodontic tooth movement appliances. Orthodontic tooth movement was initiated 8 weeks after operation and the view immediately after bonding of the appliance was shown **(A)**. Twelve weeks after orthodontic tooth movement, the tooth was moved into the grafted region and the view before sacrifice was shown **(B)**. Measurement of tooth movement using the three-dimensional scanned model: frontal view of the model **(C1)** and lateral view of the model **(C2)**. Color images available online at www.liebertonline.com/tea

a circle was drawn with the anterior point of the apertura piriformis as the center with an image analysis system (Image-Pro Plus™; Media Cybernetic). The circle was tangent to the lowest point of the alveolar crest. The radius of the circle in the occlusal films at the time immediately after bone graft implantation and 20 weeks later was measured and recorded as the height of the alveolar crest (R_0, R_1). The ratio (R) of the maintained height of the residual alveolar crest compared with the height immediately after implantation surgery was calculated using the formula: $R=(R_1\times L_0/L_1)/R_0$. A scheme was drawn to illustrate this method (Fig. 5E).

The method was adopted to reduce the interindividual angle deviations and avoid distortions possibly presented in radiographic photos.

Sequential fluorescent labeling

To observe the time course of new bone formation and mineralization, the animals were intraperitoneally injected with 25 mg/kg tetracycline (TE) hydrochloride (Sigma) at 4 weeks and 20 mg/kg calcein (CA; Sigma) at 12 weeks after the operation. Finally, 30 mg/kg alizarin red S (AL; Sigma) was administered 3 days before the animals were sacrificed at week 20 as previously described by Wang *et al.*[31]

Sample preparation and histological and histomorphometric observation

The dogs were sacrificed at 20 weeks after implantation and the premaxillas were harvested and fixed in 4% buffered

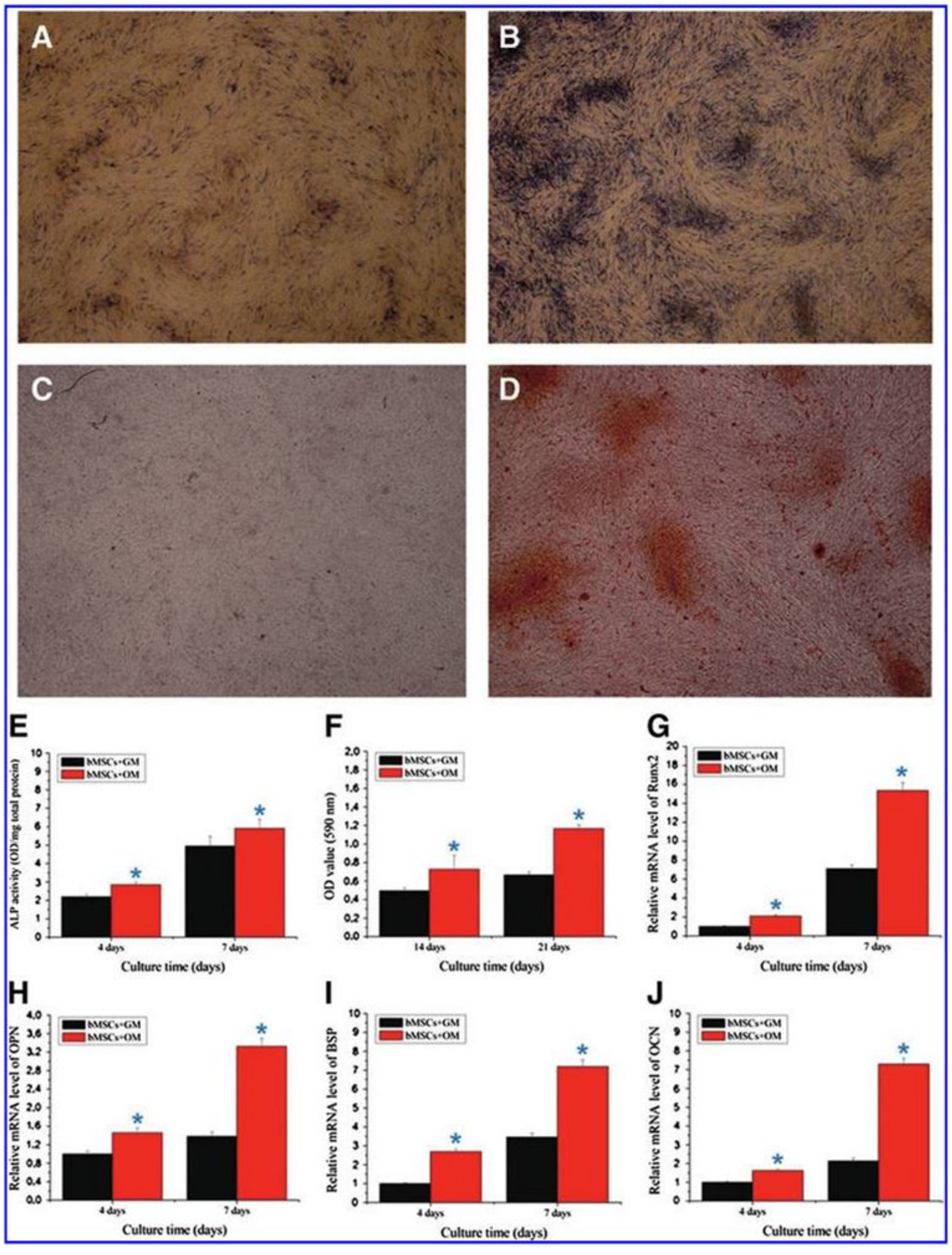

FIG. 3. Osteogenic differentiation of bone marrow stromal cells (bMSCs) cultured in the growth medium (GM) or osteogenic medium (OM). **(A, B)** Alkaline phosphatase (ALP) staining of bMSCs cultured in GM **(A)** (16×) or OM **(B)** (16×); **(C, D)** mineralized calcium nodules by alizarin red S (AL) staining in GM **(C)** (16×) or OM **(D)** (16×); **(E)** the ALP activity of bMSCs cultured in GM or OM was measured with the quantitative ALP assay; **(F)** quantitative mineral deposition by bMSCs cultured in GM or OM; **(G–J)** real-time polymerase chain reaction expression analysis of osteogenic differentiation-related genes in bMSCs cultured in GM or OM. **(G)** runt-related transcription factor 2 (Runx2); **(H)** osteopontin (OPN); **(I)** bone sialoprotein (BSP); **(J)** osteocalcin (OCN) (*significant differences between GM vs. OM; $p<0.05$). Color images available online at www.liebertonline.com/tea

paraformaldehyde (pH 7.4) for 4 days. The central parts of the samples containing the first lateral incisor and the canine were dehydrated in ascending concentrations of alcohols from 75% to 100%. Finally, the samples were embedded in polymethylmethacrylate (Sigma) for 14 days before polymerization. The specimens were cut into 150-μm-thick sections using diamond-coated internal-hole saw microtome (Leica SP1600), and were subsequently ground and polished to a final thickness of about 50 μm for the observation of fluorescent labeling using a confocal laser scanning microscope (Leica TCS Sp2 AOBS). Excitation/emission wavelengths were used as follows: 405/580 nm (TE, yellow), 488/517 nm (CA, green), and 543/617 nm (AL, red).[32]

To quantitate the bone formation and mineralization in the grafted alveolar, the fluorochrome staining of the same three locations, the top, middle, bottom of the central grafted area between the canine and the second incisor, were scanned, respectively. Five photographs were taken from the same area for each of the three positions: three fluorescence microscopy images including the fluorochromes TE, CA, and AL; one merging image of three fluorescent labeling to analyze mineralization of elevated alveolar ridge; and one image using transmission light microscopy without a specific filter combining the former merging image. Digital images of the microscope were stored and evaluated histomorphometrically using a picture-analysis system (Image-Pro Plus; Media Cybernetic). Using this system, the number of pixels labeled with each fluorochrome in each image was measured as a percentage of the mineralization area. This was done separately for yellow (TE), green (CA), and red (AL) and represented the bone formation and mineralization at the time 4, 12, and 20 weeks, postoperatively.

The undecalcified sections were further stained with Van Gieson's picro fuchsin for histological observation after fluorescent analysis. Three randomly selected sections from the serial mesio-distal sections of each sample were evaluated using image analysis system (Image-Pro Plus; Media Cybernetic). The percentage of newly formed bone and the residual β-TCP scaffold in the remaining grafted area was calculated at low magnification (12.5×).

Statistical analysis

All the data are presented as mean ± standard deviation. Statistical analysis for osteogenic differentiation was performed by independent-samples *t*-tests, whereas the differences between groups A, B, and C were analyzed by analysis of variance and Student-Newman-Keuls (SNK) *post hoc* or Kruskal–Wallis nonparametric procedure followed by Mann–Whitney *U*-test for multiple comparisons based on the normal distribution and equal variance assumption test, at a significance level of $p < 0.05$. Statistical analysis was performed using SPSS v.10.1 software (SPSS Inc.).

Results

Cell culture and osteogenic differentiation

Scattered bMSC colonies were observed after 5–7 days of culture after initial seeding, and the cells became confluent after ~10–12 days. Cells were then passaged and cultured in the growth medium or osteogenic medium. The cells cultured in the osteogenic medium demonstrated stronger ALP staining at 7 days (Fig. 3A, B), and more pronounced alizarin red staining (Fig. 3C, D) at 21 days than the cells cultured in the growth medium. The quantitative analysis of ALP activity and mineralization also indicated an increase over time with higher values under the osteogenic medium ($p < 0.05$; Fig. 3E, F). The real-time PCR results showed increased expression of osteogenic genes (*Runx2*, *OPN*, *BSP*, and *OCN*), at days 4 and 7 when cells were cultured in the osteogenic medium compared to those cultured in the growth medium ($p < 0.05$; Fig. 3G–J).

Cell seeding and osteogenic differentiation on β-TCP scaffolds

The interconnected porosity was evaluated using the SEM. The scaffolds had volume porosity of ~70% with average pore diameter of 450 ± 50 μm. The bMSCs could be seen spreading well on the inner surface of the scaffold *in vitro* 4 days after cell seeding (Fig. 4A, B). The results from the ALP activity assay, quantitative alizarin red mineralization, and quantitative real-time PCR analysis showed that the osteogenic differentiation of bMSCs on β-TCP scaffolds was significantly enhanced in the osteogenic medium as compared to the cells cultured in the growth medium. This better differentiation of bMSCs on β-TCP scaffolds under the osteogenic medium was consistent with the bMSCs cultured on Petri dishes (Fig. 4C–H). These results suggested that the biomaterial possessed favorable properties for cell attachment and differentiation and was suitable for further studies.

Gross observations and measurement of orthodontic tooth movement

All dogs heal uneventfully after surgery without infections and dehiscence of the grafted bone. There was only slight edema in the soft tissue but disappeared 2–3 days post-surgery. When orthodontic tooth movement initiated 8 weeks after surgery, spotted ulceration can be observed on the buccal mucosa due to friction with the bonded tooth movement appliances.

The first lateral incisors moved distally with a distance of 5.345 ± 0.936, 6.986 ± 1.412, and 4.665 ± 0.483 mm in groups A, B, and C, respectively. There was a significant difference between group B versus group A or C ($p < 0.05$), but no difference between group A and group C. This indicated that porous β-TCP with or without bMSCs did allow as much movement of the adjacent teeth into the repaired defects as the autologous bone.

Radiographic analyses

All the experimental areas in alveolar bone in the pre-surgery occlusal radiographs were uniform without missing teeth or pathological manifestations (Fig. 5A-1–D-1). In groups A and B, the alveolar defects were filled with radio-opaque particle materials immediately after implantation. The radiographic density of the graft sites was higher than the normal alveolar bone due to the radiopaque properties of β-TCP scaffold (Fig. 5A-2, B-2). At 4 weeks after implantation, the degradation of the grafted materials was evident, and the radio-density in the groups A and B is lower than the normal alveolar bone, indicating the resorption of the scaffolds (Fig. 5A-3, B-3). At 8 weeks, the radio-density of the

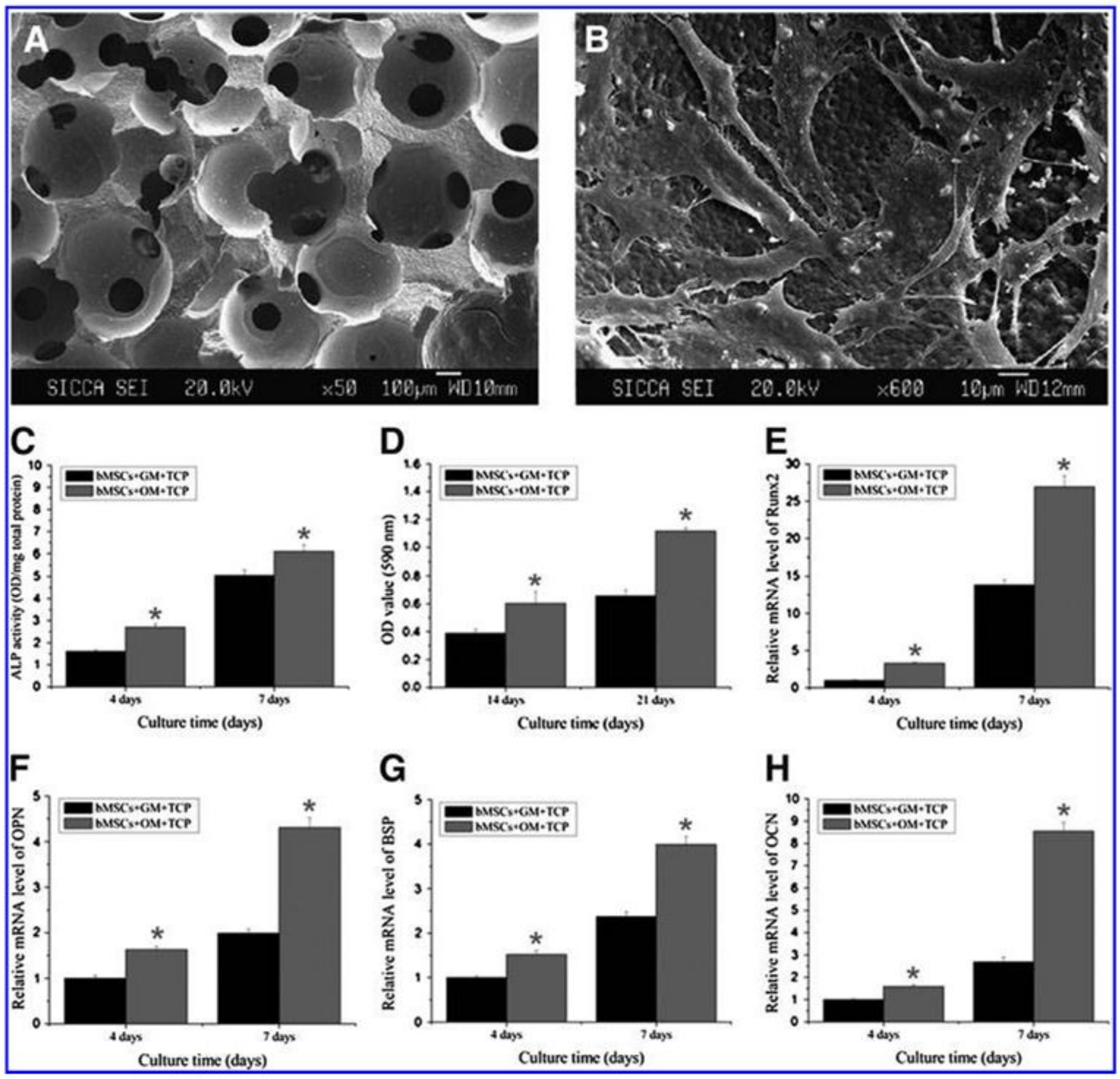

FIG. 4. Spreading and osteogenic differentiation of bMSCs on beta-tricalcium phosphate (β-TCP). **(A)** Three-dimensional porous structures of β-TCP by scanning electron microscopy (50×). **(B)** Four days after being combined with β-TCP, the bMSCs could spread well on the surface of the scaffold (600×); **(C)** the ALP activity of bMSCs seeded on β-TCP was measured with the quantitative ALP assay in GM or OM; **(D)** mineral deposition in bMSCs cultured on β-TCP under GM or OM; **(E–H)** real-time polymerase chain reaction analysis of osteogenic differentiation-related gene expression of bMSCs in GM or OM. **(E)** Runx2; **(F)** OPN; **(G)** BSP; **(H)** OCN (*significant differences between GM and OM; $p < 0.05$).

grafted area was similar to the normal alveolar bone and the contour of the surgical created defect became distinguishable in group A (Fig. 5A-4). This was indicative of the new bone formation and remolding in this defect. Only a small radiopaque area could be observed in group B, and the radiodensity of the grafted area was very low compared to the group A as well as the surrounding normal alveolar bone. The contours of the defect were clearly evident at that time (Fig. 5B-4). At 20 weeks, the first lateral incisor has been moved into the grafted area in group A. The periodontium of the tooth was considered well neither with periodontium hypertrophy nor sclerosis. There was complete bridging in the alveolar defect in this group. Cortical bone and cancellouse bone could also been seen in the defect area, making it indistinguishable from surrounding alveolar bone adjacent to the cleft (Fig. 5A-5). Although the tooth in group B has been also moved into the defect, there was not as much bone support for the tooth in the distal direction. The radiodensity of the grated area remained relatively low, making the defect distinct from the surrounding alveolar bone (Fig. 5B-5).

In group C, the density of the grafted autologous bone was lower than that of groups A and B immediately after implantation, and the texture of the grafted bone was homogenous. The radio-density increased overtime, whereas the vertical height of the alveolar bone decreased. At 8 weeks, the grafted bone possessed normal architectures of the alveolar bone and it was difficult to discriminate the implant from the defect site (Fig. 5, C). In the blank control group, there was still a highly radiolucent area with a clear contour even 20 weeks after operation (Fig. 5, D).

The ratio of the residual alveolar height was calculated using the method described above, and the value was 73.60%±6.51%, 56.31%±7.72%, and 72.42%±8.72% for groups A, B, and C, respectively. The rate was significantly ($p < 0.05$) lower in group B than in groups A and C. There was no significant difference between groups A and C, indicating that the tissue-engineered bone constructing with bMSCs/β-TCP could achieve an equivalent effect on maintaining alveolar height as the autologous bone.

Fluorochrome labeling analysis

New bone formation and mineralization at different time periods were analyzed by measuring different fluorescent labeling area. At 4 weeks after implantation, the percentage of TE labeling (yellow) in group A was 2.45%±0.82%, which was significant higher than that in group B at 1.43%±0.51% (Fig. 6A1–C1), but no significant difference was observed with group C at 1.98%±0.68% (Fig. 6D). There was also no significant difference between groups B and C (Fig. 6D). At 12 weeks, the percentage of CA labeling (green) was 2.27%±0.75%, 1.33%±0.56%, and 1.83%±0.83% for groups A, B, and C, respectively (Fig. 6A2–C2). There was significant difference between groups A and B, but no significant difference between groups A and C, or groups B and C

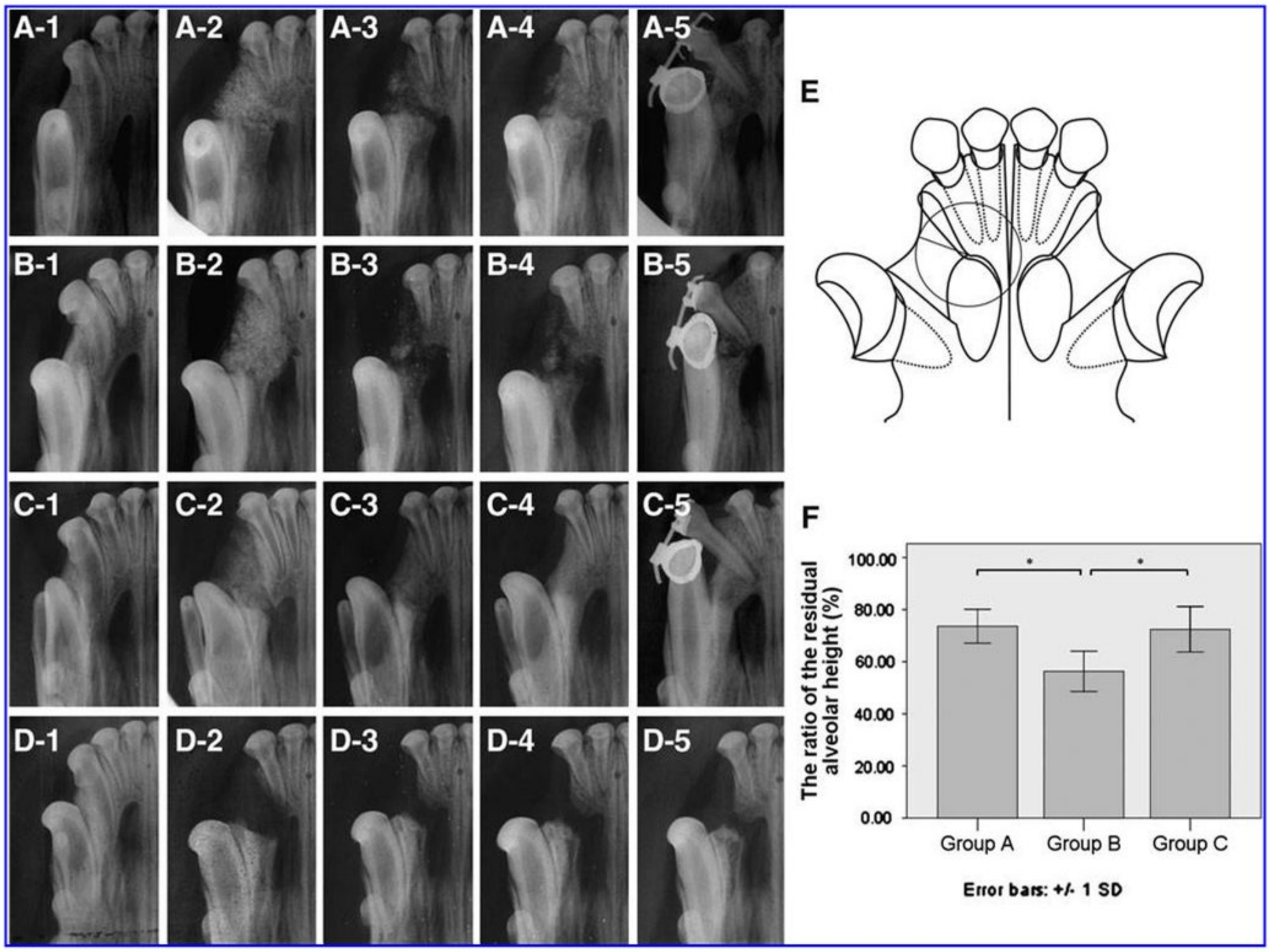

FIG. 5. Sequential occlusal radiographic findings of the repaired alveolar cleft, the images of **(A-1, B-1, C-1, D-1)**, **(A-2, B-2, C-2, D-2)**, **(A-3, B-3, C-3, D-3)**, **(A-4, B-4, C-4, D-4)**, and **(A-5, B-5, C-5, D-5)** were taken at preoperation, immediately, 4, 12, and 20 weeks after operation. A, B, C, and D represent groups A, B, and C, and the blank control group, respectively. Schematic diagram of the height measurement of the repaired alveolar from the occlusal radiograph **(E)**. The graph showed the ratio of the remained height of three different groups 20 weeks postoperatively compared with the height immediately postoperatively (*significant differences; $p<0.05$) **(F)**.

(Fig. 6D). At 20 weeks, the percentage of AL labeling (red) was 1.66%±0.60%, 0.64%±0.39%, and 0.36%±0.11%, for groups A, B, and C, respectively (Fig. 6A3–C3). There was significant difference between groups A and B, or groups A and C, but no significant difference between groups B and C (Fig. 6D). These data indicated that when bMSCs were combined with β-TCP scaffold, there was a sustained bone formation and mineralization that was higher than the β-TCP scaffold alone throughout the experimental period. The autologous iliac bone remodeled significantly at an earlier stage; as evident from the fluorescent area and intensity at the graft area, the fluorescent labeling (red) was very little at 20 weeks after implantation, indicating low bone deposition at a later period.

Histological and histomorphometric findings

Based on the light microscopy analysis of undecalcified specimens stained with Van Gieson's picro fuchsin, residual β-TCP was seen surrounded by the newly formed bone in the grafted region in groups A and B (Fig. 7A1, A2, B1, B2, C1, C2). The percentage of newly formed bone between the canine and the second lateral incisor was 54.98%±9.22% in group B, which was significantly lower than that in group A (70.79%±7.02%) and group C (78.68%±4.91%). There was no significant difference between groups A and C (Fig. 7D). The percentage of residual β-TCP in the remaining grafted region was 5.47%±1.32% in group A, and 5.17%±1.61% in group B; there was no significant difference between the two groups (Fig. 7E).

Discussion

This study was aimed at exploring whether a tissue-engineered bone from biodegradable β-TCP and bMSCs could be grafted in alveolar cleft and be as effective as a autologous bone graft for sequent orthodontic tooth movement.

Tissue engineering aims at developing substitutes for biological grafts by using scaffolds and seed cells. In the present study, bMSCs were selected as the cell source because they can be easily isolated from bone marrow aspirated from iliac crest and expanded, making large quantities

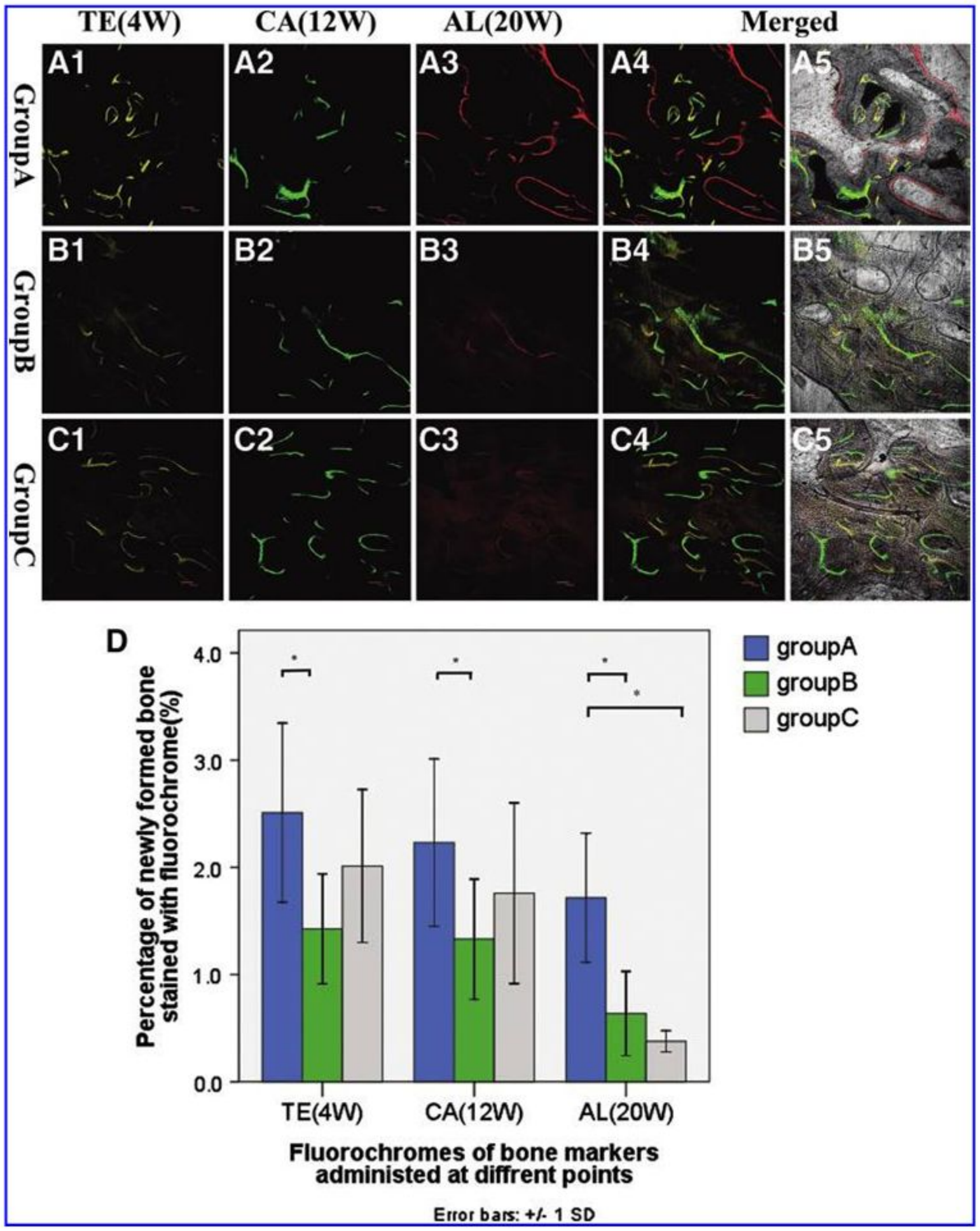

FIG. 6. Sequential fluorescent labeling of tetracycline (TE), calcein (CA), and AL administered at 4, 12, and 20 weeks separately was used to determine the rate of bone formation and mineralization. The images of **(A1, B1, C1)**, **(A2, B2, C2)**, and **(A3, B3, C3)** were labeled for 4, 12, and 20 weeks separately after operation. A, B, and C represented each group (50×). **(A4, B4,** and **C4)** represented merged images of the three fluorochromes for the same group (50×). **(A5, B5,** and **C5)** represented the merged images of the three fluorochromes together with plain confocal laser microscope image for the same group (50×). The graph shows the percentage of each fluorochrome area for different groups (*significant differences; $p < 0.05$) **(D)**. Color images available online at www.liebertonline.com/tea

available for transplantation. More importantly, based on the results of several assays intended for osteogenesis assessment (ALP activity, mineralization, and gene expression by PCR), bMSCs cultured in the osteogenic medium possessed the desired osteoblastic phenotypes, which ideally required for cells in bone regeneration.

The application of β-TCP as a clinical scaffold in repairing bone defects was well explored in recent years. Numerous studies have reported that the biocompatible and osteoconductive β-TCP scaffolds could support the attachment, proliferation, and differentiation of osteogenic cells (such as osteoblasts and bMSCs).[27,33–36] In agreement with these literatures, the microscopy analysis of the bMSCs/β-TCP constructs in this study also showed that the cells could adhere to the surface of the scaffold, spread, and proliferate. As in regular culture on tissue culture plastic, the bMSCs cultured on β-TCP scaffold displayed the expected osteogenic activity when cultured in the osteogenic medium. This was evident on all of the parameters investigated (i.e., ALP activity, mineralization, and osteogenic gene expression), and suggested that β-TCP scaffold could act as a suitable three-dimensional matrix. The β-TCP was also reported to exhibit the appropriate strength to resist complicated pressures in the oral cavity, making β-TCP a good choice for the filling of bone defects in the alveolar region.[15,31,37] Through this study, we extended the therapeutic applications of β-TCP and osteoinduced bMSCs in repairing bone defects such as alveolar cleft, specifically in supporting tooth movement in defect sites, which was attributed to the appropriate degradation of the scaffold to match with the new bone formation.

Beagle dogs were selected for this study since their periodontal structures and healing mechanisms are similar to those of humans.[16,38] It was a prerequisite that the surgically created defects in this study (10×5×15 mm, extending to the nasal floor) would not heal spontaneously during the study

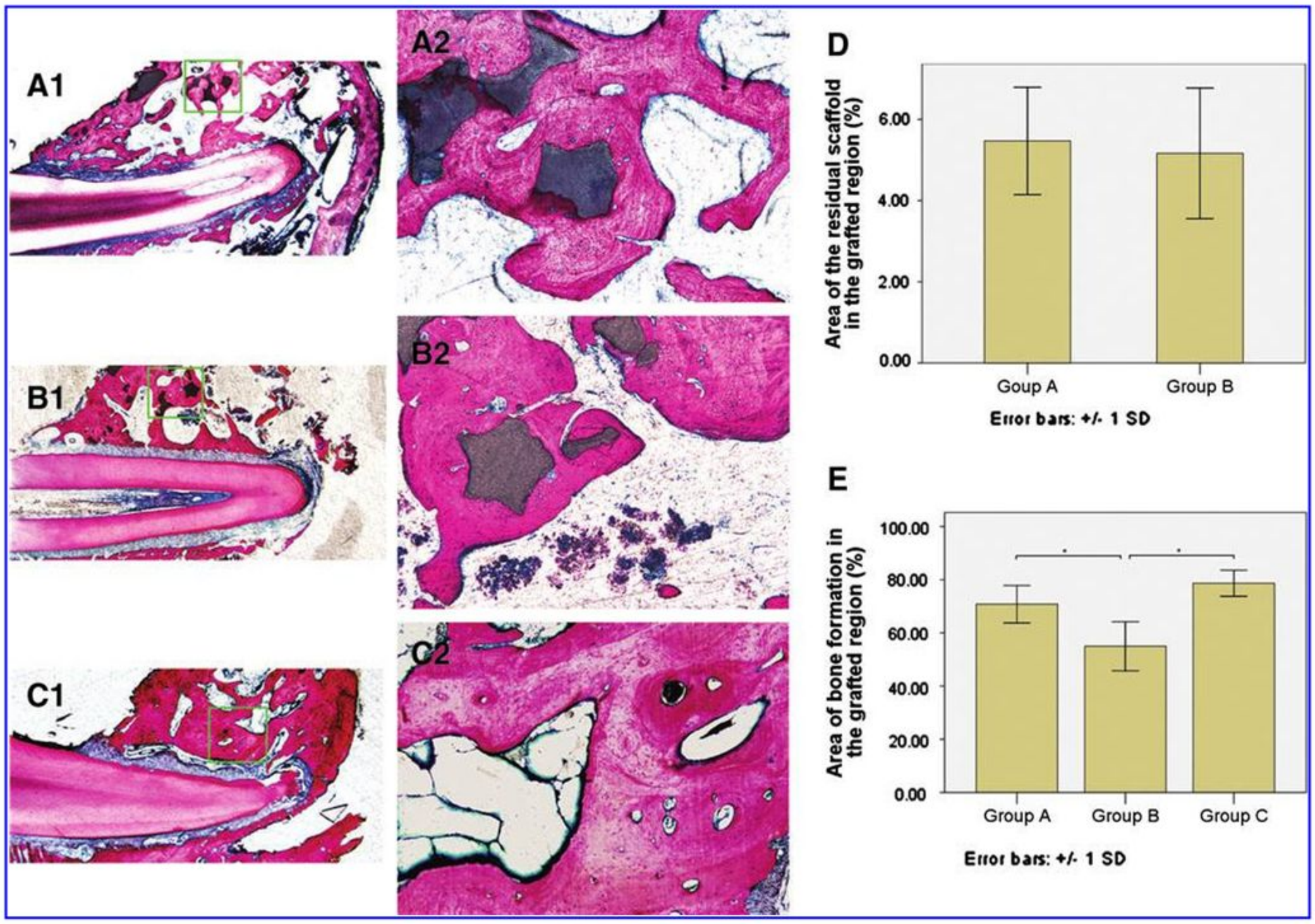

FIG. 7. Microscopic view of bone formation in the grafted area from nondecalcified slices. The images of the representative slices surrounding the orthodontic moved first lateral incisor of three groups: groups A, B, and C **(A1) (B1) (C1)** (12.5×), **(A2) (B2) (C2)** (100×) represent the high magnification for rectangle region in **A1, B1, C1,** correspondingly. The graph shows the percentage of the residual scaffold for groups A and B, and there was no significant difference between the two groups **(D)**. The graph shows the histomorphometric analysis of the new bone formation of three groups (*significant differences $p<0.05$) **(E)**. Color images available online at www.liebertonline.com/tea

period. This model was initially adopted previously by Hossain *et al.*[39] This study also confirmed the presence of highly radiolucent areas and bone discontinuity at the untreated blank controls until the end of the experiment (20 weeks), so that the defects were considered critical-sized.

In the case of alveolar cleft, an interteeth space exists between the central incisor and the canine after bone grafting so that orthodontic closure of the space is recommended for a better prognosis compared with prosthetic treatment.[13] However, orthodontic tooth movement can be performed to move the adjacent tooth into the cleft area to achieve occlusal reconstruction with patient's own teeth. Schultze-Mosgau *et al.* even reported significant lower resorption rates after bone grafting with subsequent orthodontic gap closures in comparison with gap openings (prosthodontic treatment), which suggested more favorable results for an orthodontic correction of the dental arch.[13] Some researches on orthodontic tooth movement after scaffold implantation was conducted previously.[25,39] However, those studies did not specify the reasons for the timing of orthodontic tooth movement. The previous literatures stated that orthodontic manipulation should be done 3–6 months postoperatively when the graft had already well degraded, and there was no worry for any harmful effect to the root for the moved teeth.[40,41] Based on the radiography findings in this study, most of the grafted materials already absorbed at 4 weeks after implantation, followed by obvious bone formation at 8 weeks in the tissue-engineered bone group. We therefore initiated orthodontic tooth movement at this point. The timing for initiating orthodontic tooth movement might be crucial to minimize any harm to the roots at early time points.[42] On the other hand, a late movement might cause less than desired bone formation to maintain the height of the repaired alveolar.[43,44] Whether a movement earlier than the 4 weeks (significant β-TCP degradation was noticed) might be more beneficial needs exploration in the future.

Many controversies regarding the force magnitude and duration for tooth movement are hotly debated nowadays.[45] Researchers are now inclined to accept the view that the light and continuous force was appropriate for tooth movement and periodontal health.[46] In present study, the 50 *g* orthodontic force generated by nickel–titanium coil was considered continuous and relatively light for tooth movement. After 12 weeks of orthodontic tooth movement, the first

lateral incisors were moved into the defect areas in all groups without obvious root resorption or other side effects. To determine the height of the grafted alveolar, multiple clinical and radiological schemes have been proposed.[47–51] In this study, the vertex of apertura piriformis was used as a criterion to evaluate the lowest point of the alveolar so as to establish a reproducible quantitative standard, making comparison consistent, since apertura piriformis is a relative stable anatomical landmark.

The study showed that in β-TCP group after 4 weeks, significant resorption was underwent based on the appearance of radiolucent area inside the graft. This phenomenon continued at 8 weeks with a decreased density of the grafted area. Till 20 weeks, there was only small amount augmented alveolar ridge remained with a lower radiopacity. In the tissue-engineered bone group, the resorption of the scaffold was also evident at 4 weeks; however, the radiopacity of the grafted region began to increase from week 8, and the augmented alveolar ridge maximally maintained the original height with a higher radiopacity at week 20, which was comparable to autologous bone. Although the orthodontic tooth movement was quicker in group B than in group A or C, the occlusal radiograph and sequential fluorescent labeling findings demonstrated a lower rate of bone formation and mineralization in group B than in group A, which has further led to a smaller percentage of bone area and less alveolar support to the teeth adjacent to the cleft. Since the percentage of the remaining β-TCP scaffold was similar in groups A and B, the faster tooth movement in group B was most likely due to the lower resistance with less bony support inside the defects. Unfortunately, less alveolar support in the long-term will have serious adverse effects on teeth stability in the maxillary segment.[43,47] However, β-TCP could serve as an suitable scaffold for bMSCs seeding, and the rate of bone formation and mineralization increased substantially with the incorporation of osteoinduced bMSCs. Further research is still needed to improve the effects of alveolar cleft repairing. Suitable solutions for grafting include combinations with biological molecules (i.e., bone morphogenetic proteins) to boost osteogenesis and osteoinduction in the repaired region. In addition, scaffolds that can provide more controllable degradation kinetics, such as β-TCP/HA or organic/inorganic composites, which led to better repair of alveolar cleft and improved tooth movement, might be explored in further study. As for an orthodontist, the optimal timing for orthodontic tooth movement after bone graft implantation to achieve better effect in patients with alveolar cleft is also important, since appropriate initial functional stimulation might be vital for the success of implanted bone graft.[43]

Conclusion

This study demonstrated the feasibility of using tissue-engineered bone constructs with β-TCP and bMSCs to repair alveolar cleft. The construct dramatically promoted new bone formation and mineralization, and achieved a favorable height of the repaired alveolar when compared with β-TCP implants alone, which resorbed severely during the 20-week study period. The functional effects of the tissue-engineered bone were equivalent to autologous bone and the induced tissue could support the physiological function of the alveolar by allowing the adjacent teeth to move into the newly formed bone in the grafted region. This study demonstrated that the tissue-engineered bone combining with β-TCP and bMSCs might be a feasible clinical approach as a substitute for bone grafts for patients with alveolar cleft and consequently orthodontic teeth movement.

Acknowledgments

This work was supported by National Science Foundation of China (30772431 and 30973324); Program for New Century Excellent Talents in University (NCET-08-0353); Science and Technology Commission of Shanghai Municipality (08QH14017, 08410706400, 0952nm04000, 10430710900, and 10DZ2211600); and Shanghai Education Committee (07SG19).

Disclosure Statement

No competing financial interests exist.

References

1. Waite, P.D., and Waite, D.E. Bone grafting for the alveolar cleft defect. Semin Orthod **2,** 192, 1996.
2. Lee, C., Nishihara, K., Okawachi, T., Iwashita, Y., Majima, H.J., and Nakamura, N. A quantitative radiological assessment of outcomes of autogenous bone graft combined with platelet-rich plasma in the alveolar cleft. Int J Oral Maxillofac Surg **38,** 117, 2009.
3. Boyne, P.J., and Sands, N.R. Secondary bone grafting of residual alveolar and palatal clefts. J Oral Surg **30,** 87, 1972.
4. Ishikawa, H., Kitazawa, S., Iwasaki, H., and Nakamura, S. Effects of maxillary protraction combined with chin-cap therapy in unilateral cleft lip and palate patients. Cleft Palate Craniofac J **37,** 92, 2000.
5. Kajii, T.S., Alam, M.K., and Iida, J. Orthodontic treatment of cleft lip and alveolus using secondary autogenous cancellous bone grafting: a case report. World J Orthod **10,** 67, 2009.
6. Yilmaz, S., Kilic, A.R., Keles, A., and Efeoglu, E. Reconstruction of an alveolar cleft for orthodontic tooth movement. Am J Orthod Dentofacial Orthop **117,** 156, 2000.
7. Mikoya, T., Inoue, N., Matsuzawa, Y., Totsuka, Y., Kajii, T., and Hirosawa, T. Monocortical mandibular bone grafting for reconstruction of alveolar cleft. Cleft Palate Craniofac J **47,** 454, 2010.
8. Eppley, B.L., and Sadove, A.M. Management of alveolar cleft bone grafting—state of the art. Cleft Palate Craniofac J **37,** 229, 2000.
9. Ochs, M.W. Alveolar cleft bone grafting (Part II): secondary bone grafting. J Oral Maxillofac Surg **54,** 83, 1996.
10. Gimbel, M., Ashley, R.K., Sisodia, M., Gabbay, J.S., Wasson, K.L., Heller, J., Wilson, L., Kawamoto, H.K., and Bradley, J.P. Repair of alveolar cleft defects: reduced morbidity with bone marrow stem cells in a resorbable matrix. J Craniofac Surg **18,** 895, 2007.
11. Moreau, J.L., Caccamese, J.F., Coletti, D.P., Sauk, J.J., and Fisher, J.P. Tissue engineering solutions for cleft palates. J Oral Maxillofac Surg **65,** 2503, 2007.
12. Paganelli, C., Fontana, P., Porta, F., Majorana, A., Pazzaglia, U.E., and Sapelli, P.L. Indications on suitable scaffold as carrier of stem cells in the alveoloplasty of cleft palate. J Oral Rehabil **33,** 625, 2006.

13. Schultze-Mosgau, S., Nkenke, E., Schlegel, A.K., Hirschfelder, U., and Wiltfang, J. Analysis of bone resorption after secondary alveolar cleft bone grafts before and after canine eruption in connection with orthodontic gap closure or prosthodontic treatment. J Oral Maxillofac Surg **61,** 1245, 2003.
14. Takano-Yamamoto, T., Kawakami, M., and Sakuda, M. Defects of the rat premaxilla as a model of alveolar clefts for testing bone-inductive agents. J Oral Maxillofac Surg **51,** 887, 1993.
15. Horch, H.H., Sader, R., Pautke, C., Neff, A., Deppe, H., and Kolk, A. Synthetic, pure-phase beta-tricalcium phosphate ceramic granules (Cerasorb) for bone regeneration in the reconstructive surgery of the jaws. Int J Oral Maxillofac Surg **35,** 708, 2006.
16. Linton, J.L., Sohn, B.W., Yook, J.I., and Le Geros, R.Z. Effects of calcium phosphate ceramic bone graft materials on permanent teeth eruption in beagles. Cleft Palate Craniofac J **39,** 197, 2002.
17. Kawamoto, T., Motohashi, N., Kitamura, A., Baba, Y., Takahashi, K., Suzuki, S., and Kuroda, T. A histological study on experimental tooth movement into bone induced by recombinant human bone morphogenetic protein-2 in beagle dogs. Cleft Palate Craniofac J **39,** 439, 2002.
18. Letic-Gavrilovic, A., Piattelli, A., and Abe, K. Nerve growth factor beta(NGF beta) delivery via a collagen/hydroxyapatite (Col/HAp) composite and its effects on new bone ingrowth. J Mater Sci Mater Med **14,** 95, 2003.
19. Behnia, H., Khojasteh, A., Soleimani, M., Tehranchi, A., Khoshzaban, A., Keshel, S.H., and Atashi, R. Secondary repair of alveolar clefts using human mesenchymal stem cells. Oral Surg Oral Med Oral Pathol Oral Radiol Endod **108,** e1, 2009.
20. Zaky, S.H., and Cancedda, R. Engineering craniofacial structures: facing the challenge. J Dent Res **88,** 1077, 2009.
21. He, Y., Zhang, Z.Y., Zhu, H.G., Qiu, W., Jiang, X., and Guo, W. Experimental study on reconstruction of segmental mandible defects using tissue engineered bone combined bone marrow stromal cells with three-dimensional tricalcium phosphate. J Craniofac Surg **18,** 800, 2007.
22. Yuan, J., Cui, L., Zhang, W.J., Liu, W., and Cao, Y. Repair of canine mandibular bone defects with bone marrow stromal cells and porous beta-tricalcium phosphate. Biomaterials **28,** 1005, 2007.
23. Jiang, X., Zhao, J., Wang, S., Sun, X., Zhang, X., Chen, J., Kaplan, D.L., and Zhang, Z. Mandibular repair in rats with premineralized silk scaffolds and BMP-2-modified bMSCs. Biomaterials **30,** 4522, 2009.
24. Pradel, W., Tausche, E., Gollogly, J., and Lauer, G. Spontaneous tooth eruption after alveolar cleft osteoplasty using tissue-engineered bone: a case report. Oral Surg Oral Med Oral Pathol Oral Radiol Endod **105,** 440, 2008.
25. Hibi, H., Yamada, Y., Ueda, M., and Endo, Y. Alveolar cleft osteoplasty using tissue-engineered osteogenic material. Int J Oral Maxillofac Surg **35,** 551, 2006.
26. Zhao, J., Zhang, Z., Wang, S., Sun, X., Zhang, X., Chen, J., Kaplan, D.L., and Jiang, X. Apatite-coated silk fibroin scaffolds to healing mandibular border defects in canines. Bone **45,** 517, 2009.
27. Liu, Q., Cen, L., Yin, S., Chen, L., Liu, G., Chang, J., and Cui, L. A comparative study of proliferation and osteogenic differentiation of adipose-derived stem cells on akermanite and beta-TCP ceramics. Biomaterials **29,** 4792, 2008.
28. Sun, H., Wu, C., Dai, K., Chang, J., and Tang, T. Proliferation and osteoblastic differentiation of human bone marrow-derived stromal cells on akermanite-bioactive ceramics. Biomaterials **27,** 5651, 2006.
29. Venugopal, J., Low, S., Choon, A.T., Kumar, A.B., and Ramakrishna, S. Electrospun-modified nanofibrous scaffolds for the mineralization of osteoblast cells. J Biomed Mater Res A **85,** 408, 2008.
30. Hasegawa, T., Miwa, M., Sakai, Y., Niikura, T., Lee, S.Y., Oe, K., Iwakura, T., Kurosaka, M., and Komori, T. Efficient cell-seeding into scaffolds improves bone formation. J Dent Res **89,** 854, 2010.
31. Wang, S., Zhang, Z., Zhao, J., Zhang, X., Sun, X., Xia, L., Chang, Q., Ye, D., and Jiang, X. Vertical alveolar ridge augmentation with beta-tricalcium phosphate and autologous osteoblasts in canine mandible. Biomaterials **30,** 2489, 2009.
32. Wang, S., Zhang, Z., Xia, L., Zhao, J., Sun, X., Zhang, X., Ye, D., Uludag, H., and Jiang, X. Systematic evaluation of a tissue-engineered bone for maxillary sinus augmentation in large animal canine model. Bone **46,** 91, 2010.
33. Nyangoga, H., Aguado, E., Goyenvalle, E., Basle, M.F., and Chappard, D. A non-steroidal anti-inflammatory drug (ketoprofen) does not delay beta-TCP bone graft healing. Acta Biomater **6,** 3310, 2010.
34. Walsh, W.R., Vizesi, F., Michael, D., Auld, J., Langdown, A., Oliver, R., Yu, Y., Irie, H., and Bruce, W. Beta-TCP bone graft substitutes in a bilateral rabbit tibial defect model. Biomaterials **29,** 266, 2008.
35. Clarke, S.A., Hoskins, N.L., Jordan, G.R., and Marsh, D.R. Healing of an ulnar defect using a proprietary TCP bone graft substitute, JAX, in association with autologous osteogenic cells and growth factors. Bone **40,** 939, 2007.
36. Cao, H., and Kuboyama, N. A biodegradable porous composite scaffold of PGA/beta-TCP for bone tissue engineering. Bone **46,** 386, 2009.
37. Koepp, H.E., Schorlemmer, S., Kessler, S., Brenner, R.E., Claes, L., Gunther, K.P., and Ignatius, A.A. Biocompatibility and osseointegration of beta-TCP: histomorphological and biomechanical studies in a weight-bearing sheep model. J Biomed Mater Res B Appl Biomater **70,** 209, 2004.
38. Berglundh, T., Lindhe, J., and Sterrett, J.D. Clinical and structural characteristics of periodontal tissues in young and old dogs. J Clin Periodontol **18,** 616, 1991.
39. Hossain, M.Z., Kyomen, S., and Tanne, K. Biologic responses of autogenous bone and beta-tricalcium phosphate ceramics transplanted into bone defects to orthodontic forces. Cleft Palate Craniofac J **33,** 277, 1996.
40. Bilkay, U., Tokat, C., Ozek, C., Gundogan, H., Gurler, T., Tegsel, Z., and Songur, E. Cancellous bone grafting in alveolar cleft repair: new experience. J Craniofac Surg **13,** 658, 2002.
41. Nique, T., Fonseca, R.J., Upton, L.G., and Scott, R. Particulate allogeneic bone grafts into maxillary alveolar clefts in humans: a preliminary report. J Oral Maxillofac Surg **45,** 386, 1987.
42. Cottrell, D.A., and Wolford, L.M. Long-term evaluation of the use of coralline hydroxyapatite in orthognathic surgery. J Oral Maxillofac Surg **56,** 935, 1998.
43. Dempf, R., Teltzrow, T., Kramer, F.J., and Hausamen, J.E. Alveolar bone grafting in patients with complete clefts: a comparative study between secondary and tertiary bone grafting. Cleft Palate Craniofac J **39,** 18, 2002.

44. Arangio, P., Marianetti, T.M., Tedaldi, M., Ramieri, V., and Cascone, P. Early secondary alveoloplasty in cleft lip and palate. J Craniofac Surg **19,** 1364, 2008.
45. Melsen, B. Tissue reaction to orthodontic tooth movement—a new paradigm. Eur J Orthod **23,** 671, 2001.
46. Chan, E., and Darendeliler, M.A. Physical properties of root cementum: part 5. Volumetric analysis of root resorption craters after application of light and heavy orthodontic forces. Am J Orthod Dentofacial Orthop **127,** 186, 2005.
47. Bergland, O., Semb, G., and Abyholm, F.E. Elimination of the residual alveolar cleft by secondary bone grafting and subsequent orthodontic treatment. Cleft Palate J **23,** 175, 1986.
48. Witherow, H., Cox, S., Jones, E., Carr, R., and Waterhouse, N. A new scale to assess radiographic success of secondary alveolar bone grafts. Cleft Palate Craniofac J **39,** 255, 2002.
49. Murthy, A.S., and Lehman, J.A. Evaluation of alveolar bone grafting: a survey of ACPA teams. Cleft Palate Craniofac J **42,** 99, 2005.
50. Kokkinos, P.P., Ledoux, W.R., Kinnebrew, M.C., and Weinberg, R. Iliac apophyseal cartilage augmentation of the deficient piriform rim and maxilla in alveolar cleft grafting. Am J Orthod Dentofacial Orthop **112,** 145, 1997.
51. Hynes, P.J., and Earley, M.J. Assessment of secondary alveolar bone grafting using a modification of the Bergland grading system. Br J Plast Surg **56,** 630, 2003.

Address correspondence to:
Xinquan Jiang, D.D.S., Ph.D.
Oral Bioengineering Lab
Shanghai Research Institute of Stomatology
Ninth People's Hospital Affiliated
to Shanghai Jiao Tong University
School of Medicine, Shanghai Key Laboratory of Stomatology
Shanghai 200011
China

E-mail: xinquanj@yahoo.cn

Yufen Qian, B.D.S., M.D.Sc.
Department of Orthodontics
Ninth People's Hospital Affiliated
to Shanghai Jiao Tong University
School of Medicine, Shanghai Key Laboratory
of Stomatology
Shanghai 200011
China

E-mail: yufen62004@yahoo.com.cn

Received: August 19, 2010
Accepted: January 10, 2011
Online Publication Date: March 17, 2011